Influence of Alkyl Chains of Modified Polysuccinimide-Based Polycationic Polymers on Polyplex Formation and Transfection

Marcelo H. Kravicz, Debora T. Balogh, Mrityunjoy Kar, Stefanie Wedepohl, Maria Vitoria L. B. Bentley, and Marcelo Calderón*

The development of polymers with low toxicity and efficient gene delivery remains a significant barrier of nonviral gene therapy. Modification and tuning of chemical structures of carriers is an attractive strategy for efficient nucleic acid delivery. Here, polyplexes consisting of plasmid DNA (pDNA) and dodecylated or non-dodecylated polysuccinimide (PSI)-based polycations are designed, and their transfection ability into HeLa cells is investigated by green fluorescent protein (GFP) expressing cells quantification. All cationic polymers show lower cytotoxicity than those of branched polyethyleneimine (bPEI). PSI and bPEI-based polyplexes have comparable physicochemical properties such as size and charge. Interestingly, a strong interaction between dodecylated polycations and pDNA caused by the hydrophobic moiety is observed in dodecylated PSI derivatives. Moreover, the decrease of GFP expression is associated with lower dissociation of pDNA from polyplexes according to the heparin displacement assay. Besides, a hydrophobization of PSI cationic derivatives with dodecyl side chains can modulate the integrity of polyplexes by hydrophobic interactions, increasing the binding between the polymer and the DNA. These results provide useful information for designing polyplexes with lower toxicity and greater stability and transfection performance.

1. Introduction

Gene therapy is a concept originally conceived in around 1970,[1,2] as a consequence of the exponential growth in the knowledge of human gene function, the development of more effective technologies for DNA delivery,[1] and the ability to transfer and express exogenous genes in mammalian cells.[3,4] After the approval of the first gene therapy agent in 2012 by the European Medicines Agency (EMA), this field became a prominent issue of research[5] for therapeutic, prophylactic, or diagnostic approaches related directly to the recombinant nucleic acid sequence.[6]

The strategy has expanded from the plasmid DNA (pDNA) transference to messenger RNA (mRNA), microRNA (miRNA), and small interfering RNA (siRNA),[4,7] although different therapeutic payloads require different tailor-made carriers, thus complicating preclinical development.[8] The large size of pDNA (300–400 nm of hydrodynamic diameter), for instance, is one characteristic that differs in the tailoring between RNA and DNA. Besides the physical difference, the site of action in cells also changes from siRNA to pDNA. In siRNA, the downregulation of proteins occurs in the cytoplasm, whereas pDNA delivery results in protein production, which initiates in the cell nuclei with pDNA transcription.[5] For effective pDNA delivery and transcription, polycations are good candidates providing pDNA stability and uptake by the target cells.[9]

The large size of pDNA and its short half-life in the presence of serum proteins are a challenge in nucleic acid delivery

Dr. M. H. Kravicz, Prof. M. V. L. B. Bentley
School of Pharmaceutical Sciences of Ribeirão Preto
University of São Paulo
Avenida do Café, s/n, 14040903, Ribeirão Preto, SP, Brazil

Dr. M. H. Kravicz, Prof. M. Calderón, Dr. M. Kar, Dr. S. Wedepohl
Institute of Chemistry and Biochemistry
Freie Universität Berlin
Takustraße 3, 14195 Berlin, Germany

The ORCID identification number(s) for the author(s) of this article can be found under https://doi.org/10.1002/mabi.201900117.

Dr. D. T. Balogh
São Carlos Institute of Physics
University of São Paulo
CP 369, 13560-970, São Carlos, SP, Brazil

Prof. M. Calderón
IKERBASQUE
Basque Foundation for Science
48013 Bilbao, Spain

Prof. M. Calderón
POLYMAT and Applied Chemistry Department
Faculty of Chemistry
University of the Basque Country UPV/EHU
Paseo Manuel de Lardizabal 3, 20018 Donostia-San Sebastián, Spain
E-mail: marcelo.calderon@polymat.eu

**ADVANCED
SCIENCE NEWS**

www.advancedsciencenews.com

**Macromolecular
Bioscience**

www.mbs-journal.de

as it is necessary to pack this nucleic acid into nanoparticles.[5,7] Moreover, the easy plasmid unpacking from polyplexes in the cytoplasm is necessary, so that DNA is accessible to transcription factors for gene expression.[10]

Cationic polymers can be considered perfect noncovalent interaction partners for nucleic acids, providing similar size dimensions but opposite ionic charge.[8] Frequently studied cationic polymers include poly(L-lysine), chitosan, dendritic polymers,[11,12] and polyethyleneimine (PEI).[13,14] The synthetic pentamines and hexamines in PEI are more effective in condensing DNA.[15,16] Although PEI has proven to be efficient and versatile, and clinical trials suggest that PEI-based complexes have a good safety profile, this polymer is not degradable[17] and is significantly toxic in a molecular weight-dependent manner.[7,13]

Unlike most of poly(amino acid)s that are prepared by ring-opening polymerization of N-carboxyanhydrides (NCAs), a biodegradable and water-soluble poly(aspartic acid) (PASP) can be directly obtained from alkaline hydrolysis of poly(succinimide) (PSI),[18] which is a poly(imide) obtained from thermal polycondensation of aspartic acid (ASP).[19,20] Aminolysis of PSI with nucleophilic amine-bearing compounds is used to form various poly(asparamide)s with side groups like isopropylasparamides segments, thus obtaining a thermoreversible phase transition polymer,[19] biodegradable water-soluble polymeric materials,[21]

reversible micelles,[22] PEI-mimetic polymers,[20] and pseudo-branched PEI.[23] These copolymers can form aggregates, micelle-like structures,[24–26] and can be used as drug and gene delivery systems.[27,28]

Protonable nitrogens within amine groups have been identified as main components in the rational design of nonviral vectors for gene delivery[29] such as cationic polymers that can be combined with DNA to form a particulate complex, condensing and shielding the DNA from enzymatic degradation.[29] Although polymer binding the DNA requires sufficient charge, excess of positive charges leads to high-levels of cytotoxicity due to unspecific interactions with serum molecules or cellular membranes.[29]

Polymer hydrophobicity is frequently an underappreciated factor for successful gene delivery despite of its role in improving DNA binding through strengthening interactions with genetic material and interaction with cell membranes.[16,30,31] Biodegradable amphiphilic copolymers with hydrophobic moieties have been synthesized by partial aminolysis of PSI with dodecylamine and propylamine for aggregates formation.[32] Studies of O'Keeffe et al. (2018),[30] for instance, showed an increased DNA binding in their dodecylated derivatives compared to their non-dodecylated counterparts resulting in higher gene transfection efficiency. Since hydrophobic interactions play a significant role in polymer binding strength,[33]
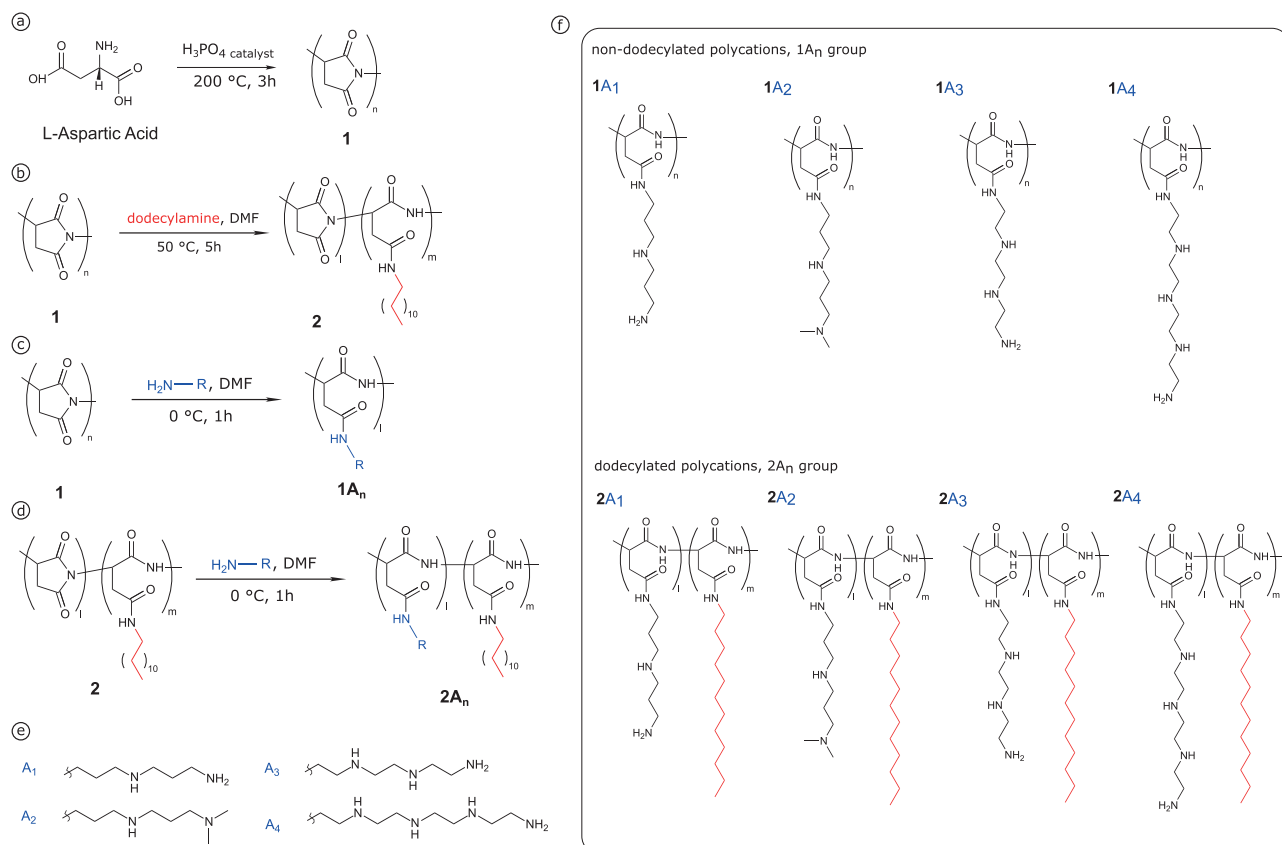

Figure 1. Synthesis of PSI derivatives. a) Synthesis of PSI (**1**) from L-ASP. b) Synthesis of dodecylated PSI (**2**), degree of substitution (DS) 10 mol%. c) Synthesis of dodecylated PSI (**2**). d) Synthesis of dodecylated PSI polycations. e) Amines A_n used for aminolysis of **1** and dodecylated PSI (**2**), thus obtaining polycations $1A_n$ and $2An$. f) Non-dodecylated PSI derivatives ($1A_n$ group) and their dodecylated counterparts ($2A_n$). The dodecyl side chain is represented in red in the copolymers.

aggregation,[19] stacking of nucleotide bases in double-strand DNA,[34] the dodecyl side chain has an influence in the binding process and gene expression in gene therapy with polyplexes.[30] DNA binding with a polycation is described as a coacervate, a complex of polyelectrolytes[35] and is mainly formed via electrostatic interactions. Moreover, a higher degree of interaction with the plasmid via Van der Waal's interactions/modulation has been reported to facilitate interactions between the polymer backbones and DNA in previous studies.[33]

Here, we synthesized a systematic series of hydrophobically modified PSI polycations to screen efficient complexing agents and to investigate their binding behavior in plasmid DNA delivery. PSI was grafted with dodecylamine and then reacted with different amine moieties, which provided non-dodecylated and dodecylated cationic polymers. Plasmid activity was screened via green fluorescent protein (GFP) expression after pEGFP-N3 plasmid complexation and transfection in HeLa cells.

2. Results and Discussion

2.1. Polymers Synthesis and Characterization

To elucidate the ability of polyplex formation of dodecylated and non-dodecylated PSI derivatives, we synthesized a series of polycations with different amine moieties. **Figure 1** presents the synthesis of PSI derivatives along with the synthesized PSI grafted with cationic moieties ($1A_n$ group, non-dodecylated polycations) and dodecylated PSI derivatives with cationic moieties ($2A_n$ group).

PSI (1) is a poly(imide), a precursor for PASP, a biodegradable and biocompatible polymer as poly(γ-glutamic) acid and poly(ε-lysine). **Table 1** shows all chemical shifts of PSI and PSI derivatives, and the spectra are presented in Figures S1–S5, Supporting Information. PSI synthesis is confirmed with three characteristic peaks in 3.2 and 2.69 ppm (methylene) and 5.25 ppm (methine), related to the succinimide ring.[19,32]

Table 2 provides the ratio (R) between dodecyl side chains and amines and the degree of substitution of grafted amines A_n (DS_A). The partial aminolysis of PSI units with dodecylamine (10 mol%) and the total ring opening of PSI units would result

Table 1. ^1H NMR chemical shifts of PSI (**1**), dodecylated PSI (**2**), and polycationic polymer groups $1A_n$ and $2A_n$.

Nucleus	^1H NMR shift [ppm]	Attribution
a	5.25	t, 1H
b	2.69 and 3.2	s, 2H
c	2.8	—
d	1.5	s, 2H
e	1.17	s, 18H
f	0.86	s, 3H
g	1.65	s, 4H
h	2.13	s, 6H
i	2.17–2.25	—

Table 2. Ratio (R) in mol% of dodecylamine (C_{12}) and cationic moieties in $2A_n$ PSI derivatives.

Polycation	$2A_1$	$2A_2$	$2A_3$	$2A_4$
R, [mol%] x (C_{12}):γ (A_n)	0.22:1	0.24:1	0.33:1	0.29:1
DS_{C12} [mol%][a]	18	19	24	22
PSI[b] (opened rings), [mol%]	10	—	—	—
DS_{C12}[c] [mol%]	8	9	14	12
DS_A[d] [mol%]	82	81	76	88

[a]Degree of substitution (DS_{C12}) in mol% calculated from the ratio obtained after total aminolysis of dodecylated PSI. Value based on ^1H NMR analysis; [b]Feed ratio of dodecylamine (theoretical); [c]Actual ratio of dodecylamine. Value based on ^1H NMR analysis; [d]Actual DS_A in mol% in $2A_n$ polycations. Value based on ^1H NMR analysis.

in a new signal at 4.5 ppm assigned to the methine proton of *N*-dodecylamide units, as observed in previous studies.[32]

For this study, the actual dodecylamine ratio found was ≈12 mol% and both PSI and its dodecylated copolymers grafted with amines A_n resulted in a total aminolysis and ring opening of PSI backbone, observed with the chemical shift of methine protons signal at 5.25 ppm to a new signal at 4.5 ppm. DS of dodecylated PSI was obtained from the integrated area ratio of the signals at 0.89 and 5.25 ppm, assigned to the methyl group of the dodecyl side chain and the methine of succinimide unit, respectively. As partial or complete racemization is expected to occur during the PSI synthesis, grafted PSI shows the split NMR signals due to the stereoregularity differences, and the disappearance of peak at 5.25 ppm and two chemical shifts values of methine protons at 4.5 were caused by an α- and β-ring opening.[36,37]

Moreover, high grafting ratios were successfully achieved with aminolysis of PSI and dodecylated PSI (**2**) and the ring opening α:β ratio was calculated from the integral area ratios of methine peaks at 4.65 (α-CH) to 4.48 ppm (β-CH).[23] **Table 3** shows the different ratios for the PSI derivatives and the α-opening predominance, as observed in previous studies with PSI grafted with bPEI.[23] Mole ratios were calculated by integrating the peaks 4.65 and 4.48 ppm.

We determined the molecular weights of the polymers by size exclusion chromatography (SEC) analysis. Here, non-dodecylated polymer group had higher weight average molecular weight (M_w) values than $2A_n$ (**Table 4**) presumably due to the hydrophobic intra- and intermolecular interactions of dodecylated polymers and fewer interactions with water molecules. The polydispersity index (PDI) of all non-dodecylated PSI derivatives (polycations group $1A_n$) did not show a clear trend

Table 3. α- and β-opening of succinimide rings of PSI (**1**) and dodecylated PSI (**2**) in the polycation groups $1A_n$ and $2A_n$ after total aminolysis process.

	$1A_n$ group				$2A_n$ group			
	$1A_1$	$1A_1$	$1A_3$	$1A_4$	$2A_1$	$2A_2$	$2A_3$	$2A_4$
α	0.8	0.8	0.67	0.7	0.68	0.70	0.47	0.54
β	0.17	0.19	0.33	0.3	0.28	0.28	0.50	0.42
α:β	4:1	4:1	2:1	2:1	2.5:1	2.5:1	1:1	1:1

**ADVANCED
SCIENCE NEWS**
www.advancedsciencenews.com

**Macromolecular
Bioscience**
www.mbs-journal.de

Table 4. Characteristics of PSI derivatives.

	M_w	M_n	M_z	PDI	N%	N	β	CMC
Non-dodecylated polycations								
1A₁	16.1	7.4	46.4	2.2	9.83	70.2	39.30	1
1A₂	19.6	9.7	34.5	2.0	7.7	55	32.92	1.03
1A₃	17.3	7.2	35.6	2.4	11.54	82.4	66.96	0.62
1A₄	25.7	9.4	57.5	2.7	12.61	90.1	40.20	0.64
	M_w	M_n	M_z	PDI	N%	N	β	CMC
Dodecylated polycations								
2A₁	8.6	2.7	19.8	3.0	6.14	43.9	41.28	0.5
2A₂	5.4	2.2	10.8	2.4	5.16	36.9	49.12	0.27
2A₃	5.5	2.2	12.3	2.5	7.61	54.4	49.96	0.22
2A₄	8.1	1.9	11.4	4.3	8.39	59.9	60.43	0.24

Molecular weights and molecular weight distributions were determined by GPC and elemental analysis (EA) was performed for the determination of total nitrogen amount (N%) and nitrogen content in 10 mg polymer (N, μmol); bPEI 25 values N% 31.89 (3.19 μmol). Buffering capacity (β, %) of PSI polycations and bPEI 25 in the pH range 7.4–5.1 (β for bPEI 25, 23.85%). Critical micellar concentration (CMC) values of dodecylated and non-dodecylated PSI derivatives, mg mL^{-1}. For convenience, we described the 1:3 ratio as I_3/I_1 ratio versus log of polymer concentration. M_w, weight-average molecular weight (kDa); M_n, number-average molecular weight (kDa); M_z, volume-average molecular weight (kDa). PDI = weight-average molecular weight/number-average molecular weight, or M_w/M_n.

with the selected amine used for the PSI grafting. The same behavior was not found for the 2A$_n$ group, in which a distribution of PDI values was found from 2 to 4. Moreover, the PDI values increased with the presence of the alkyl chain.

The polymers were titrated with HCl to obtain buffering capacity (β) profiles (**Figure 2**). In this measurement, polymers with a higher buffering capacity need larger amounts of HCl for their pH alteration. A reduction of buffering capacity is frequently associated with hydrophobic modifications.[38,39] The decrease or increase of buffering capacity is highly associated with conjugation strategies used in the grafting of PEI, since conjugation methods, in that case, lead to a conversion of surface primary amines to secondary amines, thus reducing the buffering capacity.[39] Here, the hydrophobization of PSI backbone led to substantial increase in the buffering capacity of polymers. Besides, non-dodecylated and dodecylated PSI derivatives had higher values than bPEI 25 (about 24%), the same value observed previously.[40]

As shown in Figure 2, the grafting of the dodecyl group in the PSI backbone structure changed the buffering capacity profile of PSI derivatives. Dodecylation in A₂- and A₄-based PSI derivatives provided substantial changes in the buffering profile, as also observed in Table 4. Buffering capacity values were higher for all polymers except for 2A₃ and 2A₁, the latter with a slightly lower value when compared with its non-dodecylated
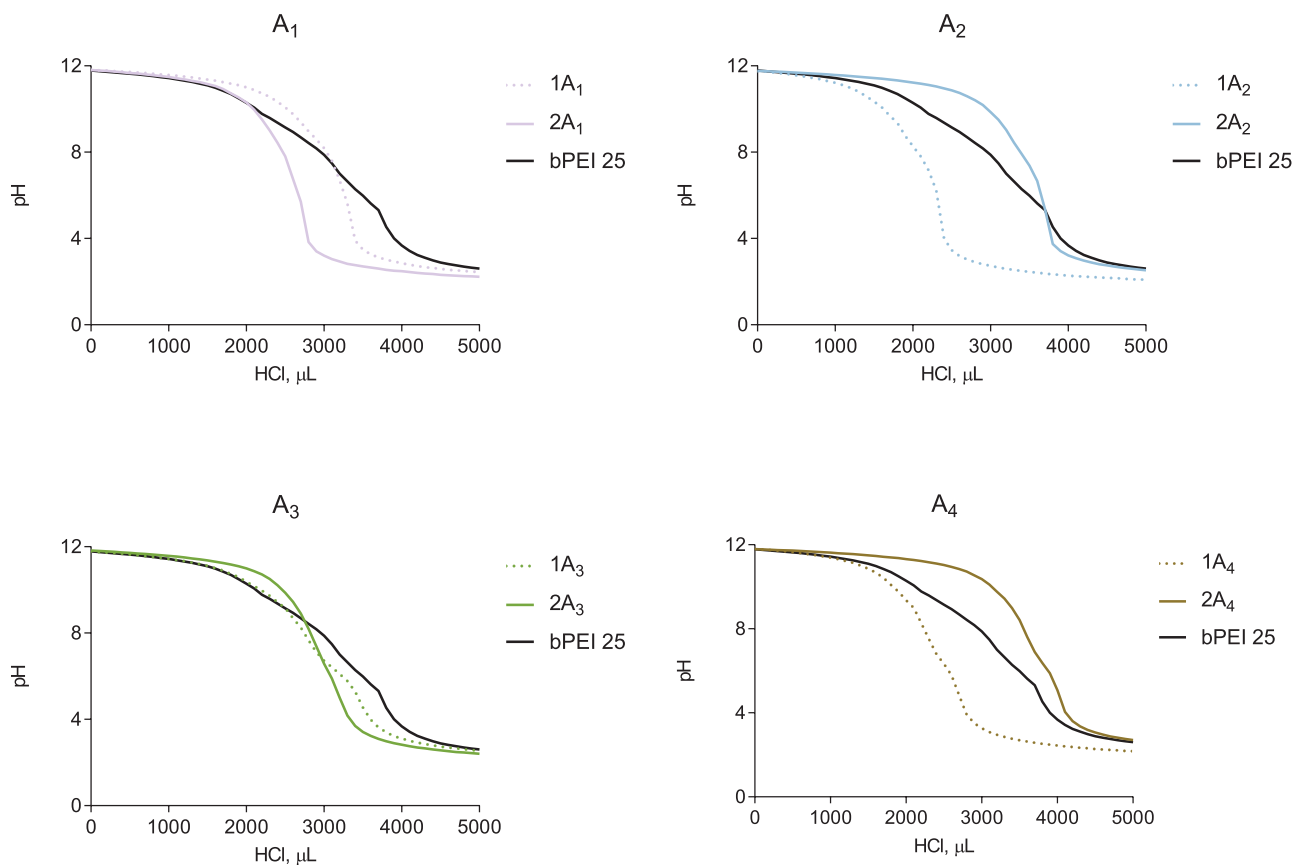

Figure 2. Acid–base titration profiles of PSI derivatives 1A$_n$ and 2A$_n$ groups in 150 mM NaCl solution. The difference between groups is the presence of a dodecylamine side chain (DS 12 mol%) in the PSI backbone of 2A$_n$ polycations group. bPEI 25 was used as a control.
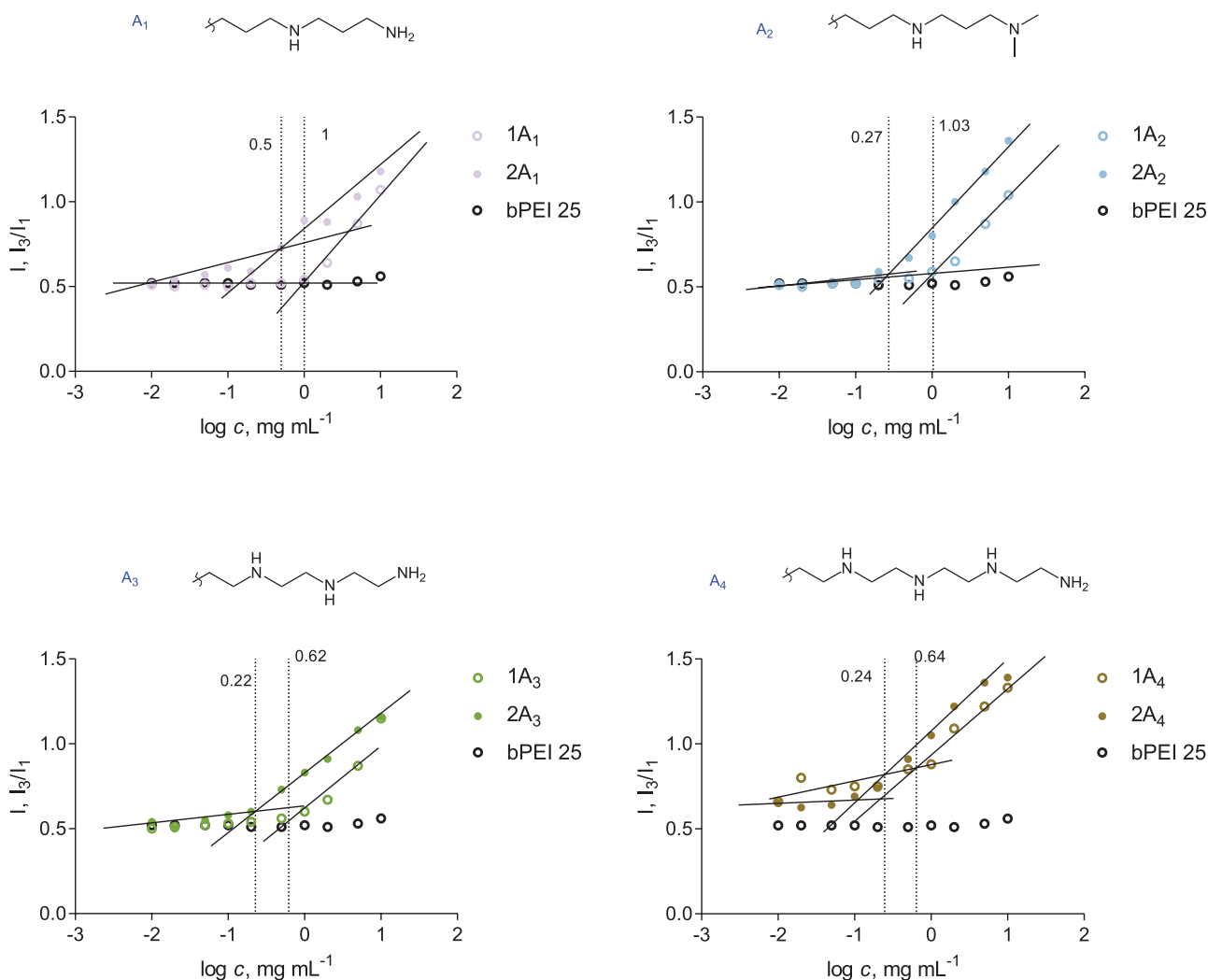
Figure 3. CMC of dodecylated and non-dodecylated PSI-based polycations. Grid lines show CMC of $1A_1$, 1 mg mL^{-1} and $2A_1$, 0.5 mg mL^{-1}; $1A_2$, 1.03 mg mL^{-1} and $2A_2$, 0.27 mg mL^{-1}; $1A_3$, 0.62 mg mL^{-1} and $2A_3$, 0.22 mg mL^{-1}; $1A_4$, 0.64 mg mL^{-1} and $2A_4$, 0.24 mg mL^{-1}. For convenience, we described the 1:3 ratio as I_3/I_1 ratio versus log of polymer concentration.

counterpart. Also, the presence of the dodecyl side chain in the backbone of $2A_3$ derivative had decreased the buffering capacity of the derivative, suggesting a dual control of hydrophobicity and amine moiety in the buffering capacity.

Ong et al. (2018) suggest in their studies that a longer and thus more hydrophobic alkyl moiety grafted in a polymer backbone contributes to a higher degree of interactions with DNA molecules possibly via Van der Waals interactions.[33] A low level of long hydrophobic substitutions such as dodecyl moieties may be sufficient to facilitate stronger hydrophobic interactions, inducing inter and intra hydrophobic–hydrophobic associations,[41,42] and changing the overall available protonable amine in the polymer, since the latter would be in a micelle-like state during the measurement. A dynamic protonation state might change the overall charge in the polymers[41] and modulate the orientation of protonable amines.

Previous studies related endosomal escape of polyplexes to the buffering effect associated to the amino groups in the constituent polycations and proton sponge hypothesis,[43] thus it is recommended that the buffering capacity might need to be balanced by controlling the type of amine and the size and degree of substitution of alkyl side chain, with all other polymer properties.[10] It is also indicated that the proper reduction of buffer capability could enhance the in vitro transfection efficiency, as DNA could be released easily from the complexes.[20]

The critical micellar concentration (CMC) of all PSI derivatives and bPEI 25 was determined (**Figure 3**). It is known that increasing the hydrophobicity of a polymer chain to a certain degree would facilitate micellization of amphiphilic polymers and a minimal hydrophobicity is indicated for bPEI 25.[44] Here, the CMC of all polycations $1A_n$ and $2A_n$ was determined according to previous studies,[45,46] and for convenience, we describe the 1:3 ratio as I_3/I_1 ratio versus log of polymer concentration. Micellar formation occurred in lower polymer concentrations in the case of the $2A_n$ group. bPEI 25 was used as a standard complexing agent and its CMC could not be
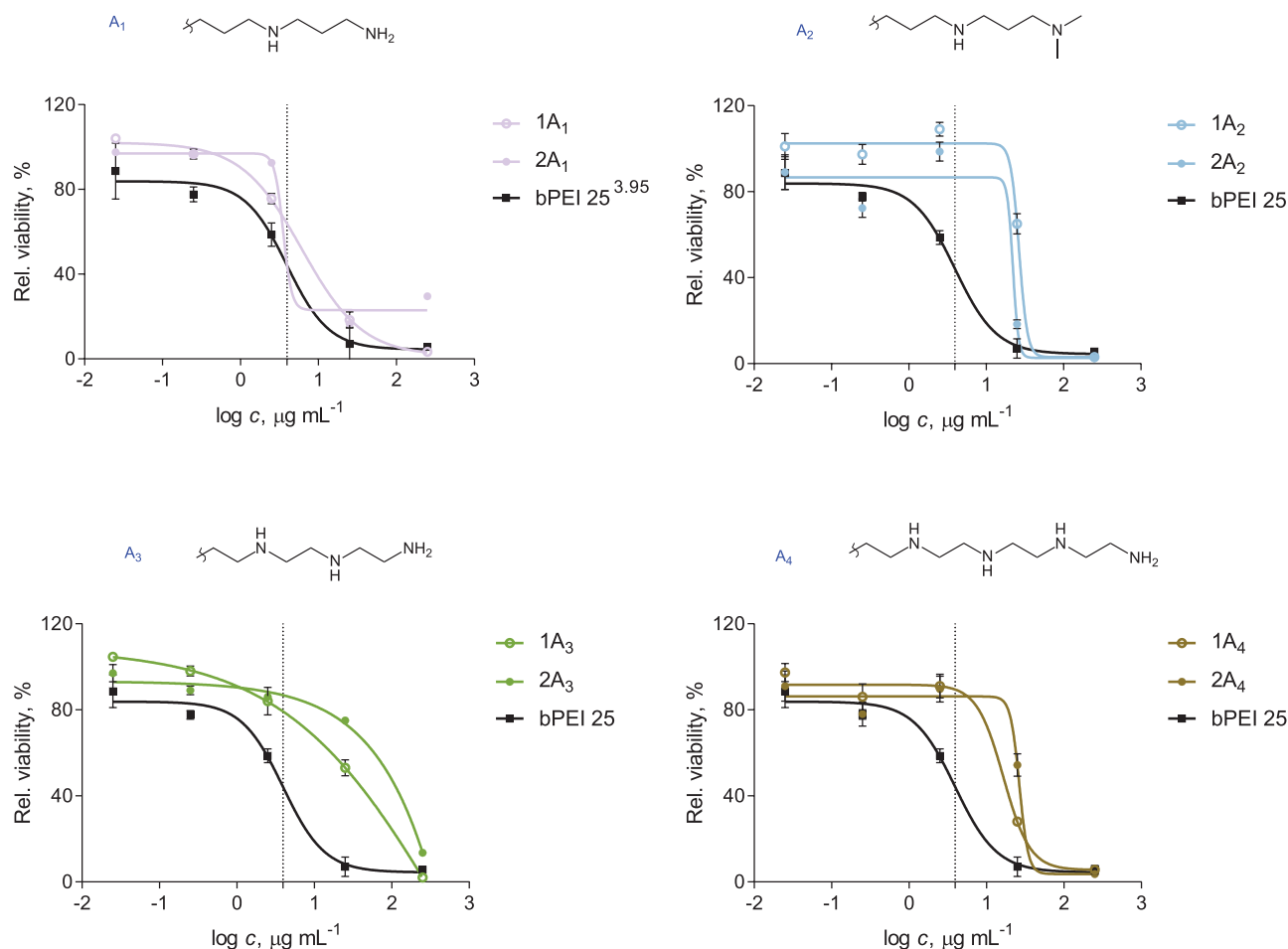
**ADVANCED
SCIENCE NEWS**
www.advancedsciencenews.com

**Macromolecular
Bioscience**
www.mbs-journal.de

Figure 4. Cytotoxicity of bare PSI derivatives in HeLa cells. Cells were treated with increasing polymer solution until 250 µg mL^{-1}. Grid line represents IC$_{50}$ 3.95 µg mL^{-1} for bPEI 25. Error bars represent the s.d. (n = 3).

detected.[44,47] Increasing the hydrophobicity of PSI backbone with alkyl segments to a certain degree facilitated micellization of amphiphilic polymers.[28]

Cytotoxicity of all polycations was concentration-dependent (**Figure 4**). The presence of the hydrophobic dodecyl side chain in the PSI backbone did not decrease the cell viability up to a concentration of 250 µg mL^{-1}, suggesting that the hydrophobic moieties do not increase cytotoxicity in the range of polymer concentrations. To confirm the non-toxicity of the alkyl chain in the polymers, cytotoxicity assays of bare dodecylated PSI derivatives obtained after amylolysis with amines 1-(3-aminopropyl) imidazole (A$_5$) and 1-(2-aminoethyl) piperazine (A$_6$) were performed (Figure S6, Supporting Information). Both imidazole and piperazine have lower in vitro cytotoxicity and are used in polymer and drug design.[48–50] For the imidazole side chain (A$_5$), higher cell viability was obtained until 250 µg mL^{-1}, and a decreased cell viability was observed for the piperazine side group (A$_6$), presumably due to the secondary amine in the piperazine ring.

For polycations of A$_3$ and A$_4$ group, increased toxicity was observed, clearly dependent on the increase of polymer concentration. Both amines are ethyleneimine-based structures, PEI components, although PSI derivatives with those amines had

lower toxicity than bPEI in the concentration range from 0.025 to 25 µg mL^{-1} and from 0.025 to 2.5 µg mL^{-1} for A$_3$ and A$_4$ grafted PSI, respectively. For transfection assays, the concentration range was between 2 and 20 µg mL^{-1}.

2.2. Physicochemical Properties and DNA Binding Ability

All PSI derivatives were mixed with plasmid DNA (pEGFP-N3) and the DNA condensation ability of each polymer at different N/P ratios was studied by gel retardation assay. The extent of condensed pEGFP-N3 is a determining factor in different transfection efficiencies in PEI-based polyplexes,[51] and inhibition of transcription can occur either if the plasmid is tightly or loosely condensed.[52]

According to the gel retardation assay (**Figure 5**a–d), an optimal N:P ratio of 2 was obtained for A$_2$- and A$_3$-based PSI polycations, and an N:P 5 for A$_1$ and A$_4$ derivatives. Both 1A$_2$ and 2A$_2$ structures differ from the A$_1$ group on two methyl end groups in the A$_2$ moiety, providing more interactions with pEGFP-N3 plasmid via hydrophobic binding, decreasing the N:P ratio. Despite the fact of fewer aminoethylene repeats in the side chain of polycations, 1A$_3$-based polyplexes were
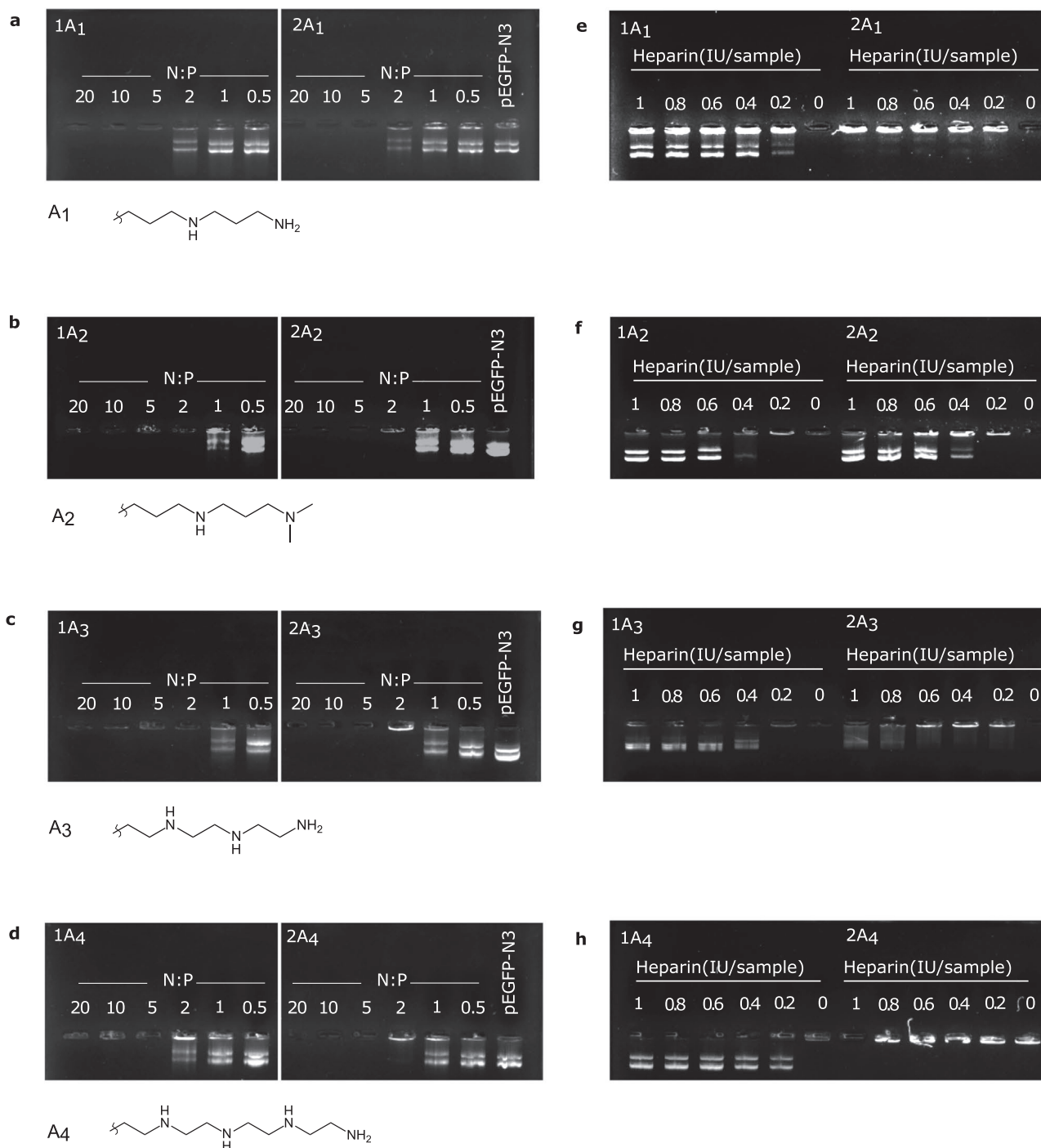
Figure 5. Evaluation of plasmid DNA binding ability and binding strength of cationic PSI derivatives. a–d) Electrophoretic mobility of pEGFP-N3 plasmid in pEGFP-N3/$1A_n$ and pEGFP-N3/$2A_n$ polyplexes at N:P 0.5–20, and e–h) displacement of pEGFP-N3 from the polyplex with increasing concentrations of heparin from 0.2 to 1 IU.

formed at lower N:P than those obtained with polycation $1A_4$. Both amines share the same protonation status at pH 7.2 with two protonated amino groups per side chain.[53] Dodecylated A_3- and A_4-based polyplexes were formed at the same N:P ratio of 2.

To evaluate the binding strength of PSI derivatives and polyplex integrity, heparin displacement assay was performed.

In this experiment, the amount of uncomplexed plasmid is accessed once free double-stranded DNA can be detected after displacement of DNA from polyplexes by different concentrations of heparin using a commonly described method.[54] For bPEI 25, the optimal complexation ratio is N:P 5, and pEGFP-N3 was displaced by heparin from concentrations above 0.6 IU per sample (Figure S7, Supporting Information).

Figure 5e–h shows that fluorescent intensities for all non-dodecylated-based polyplexes slightly increased at low heparin concentrations with a rise above 0.4–0.6 IU per sample. At 1 IU per sample, a complete displacement from the pEGFP-N3/1A$_n$ polyplexes is observed. Interestingly, fluorescence intensities for all dodecylated polyplexes at N:P 5 significantly decreased at all heparin concentrations, except for amine A$_2$.

These results suggest that the hydrophobic alkyl moieties present in the side chains of PSI contributed to the increase of polymer/DNA polyplexes interaction[55] via Van der Waal's interactions/modulation, which have been reported to facilitate interactions between the polymer backbones and DNA in previous studies.[33] Although an efficient gene delivery can be observed in polyplexes with strong pDNA binding via hydrogen bonding,[54] the presence of an alkyl chain can modulate the integrity of polyplexes by hydrophobic interactions, increasing the binding between the polymer and the DNA.

Size and surface charge of polyplexes were determined by DLS and zeta potential measurements. Size and residual charge measurements of bPEI 25 polyplexes were performed (Figure S8, Supporting Information). The size of the complexes for all N:P ratios was around 100 nm, although the polydispersion index (PDI) is optimal at N:P 5 for these polyplexes, as observed in **Figure 6**a–d.

The presence of the dodecyl side chain in the PSI derivatives did not change the size of the polyplexes obtained from PSI grafted with amine A$_1$ and A$_2$. Both groups present similar values for size and the same PDI profile with an optimal N:P ratio of 5. However, for the A$_3$ grafted PSI, polyplex sizes of the 2A$_n$ group were smaller than those from 1A$_n$, from N:P ratio 0.5 to 1. The opposite was observed for N:P ratios higher than 2, in which pEGFP-N3/2A$_3$ polyplexes had larger sizes than pEGFP-N3/1A$_3$ polyplexes. PDI values were also optimal at N:P ratios of 5 and 10. Furthermore, at N:P 2 large aggregate formation was observed, possibly due to a decreased colloidal stability induced by charge neutralization for all polyplexes. pEGFP-N3/2A$_4$ polyplexes had a lower size than pEGFP-N3/1A$_4$ at N:P ratios 0.5 and 1 with high PDI. From N:P 5, this behavior changes and pEGFP-N3/1A$_4$ particles had smaller sizes than pEGFP-N3/2A$_4$. PDI values for all polyplexes reduced as N:P ratio increased.

Regarding zeta potential measurements (Figure 6e–h), particles with a zeta potential higher than 30 mV are physically more stable due to the presence of electrostatic repulsion.[55] Zeta potential values of pEGFP-N3/bPEI25, pEGFP-N3/1A$_n$, and pEGFP-N3/2A$_n$ polyplexes have a charge inversion between N:P ratios 0.5 and 1, from a negatively to a positively charged polyplex.

2.3. Cytotoxicity of Polyplexes

In vitro transfection and GFP expression assays showed N:P 5 as optimal ratio for transfection for synthesized polycations. For all polymers, an N:P 5 was chosen for the assessment of the viability of HeLa cells after treatment with polyplexes using the MTT assay, in which polyplex volumes ranged from 25 to 100 µL, the same volumes used for transfection assays. **Figure 7** presents the viability of HeLa cells after polyplex

treatment. As expected, lower polyplexes volumes 25 and 50 µL caused no change in the cell viability in all polyplexes with synthesized dodecylated and non-dodecylated PSI derivatives or bPEI 25. Cell toxicity slightly increased for higher volumes 75 and 100 µL of dodecylated PSI derivative polyplexes, suggesting an increase of cell cytotoxicity due to the excess of free amines in the polyplexes after hydrophobic intra- and intermolecular polymer–polymer and polymer–pDNA interactions.

2.4. In Vitro Transfection Efficiency of pEGFP-N3/1A$_n$ and pEGFP-N3/2A$_n$ Polyplexes

In vitro transfection efficiency of all polyplexes was assessed to find the optimal PSI derivative among non-dodecylated and dodecylated synthesized polycations. Here, HeLa cells were treated with polyplexes in serum-free medium for 6 h and then left for another 42 h in complete medium until quantification of GFP expression by flow cytometry. To optimize the pEGFP-N3 transfection and GFP expression in HeLa cells, a series of pEGFP-N3/bPEI 25 polyplexes in different ratios and volumes was prepared (Figure S7, Supporting Information). A volume of 25 µL of pEGFP-N3/bPEI 25 N:P 5 polyplexes was considered to be the optimal transfection ratio and volume for HeLa cells transfection and GFP expression.

A dose of polyplexes and N:P ratio variation was undertaken to understand further both polyplex amount and the optimal ratio between polycation and the plasmid in the transfection efficiency, which directly play a role in the GFP expression inside the cells. Figures S10–S13 (Supporting Information) demonstrate the entire panel with transfection ability of all non-dodecylated and dodecylated polycations.

The percentage of GFP expressing HeLa cells after transfection with pEGFP-N3/1A$_4$ polyplexes was the highest among non-dodecylated and dodecylated polycations (≈48% compared to ≈20% of bPEI 25 at the same conditions, N:P 5 and 50 µL polyplex volume) (**Figure 8**). Previous studies showed that A$_4$ amine possessing even-numbered repeating aminoethylene units provided significantly higher transfection efficiencies than odd-numbered repeating units such as A$_3$ in Huh-7, A549 and HUVEC cells.[43] In our studies with HeLa cells, pEGFP-N3/1A$_3$ polyplexes also provided lower GFP expressing HeLa cells percentage than A$_4$-based non-dodecylated polycation. pEGFP-N3/1A$_3$ polyplexes showed higher GFP expressing cells at N:P 10 and 100 µL (≈42% compared to ≈4.5% of bPEI 25). In previous studies, Uchida et al.[43] associated the precise spacing between protonated amino groups in A$_3$ and A$_4$ structures to be essential for facilitating the transport of polyplexes into the cytoplasm.

The percentage of GFP expressing HeLa cells after pEGFP-N3/1A$_1$ transfection was the highest among non-dodecylated and dodecylated A$_1$ and A$_2$-based polycations (≈13% compared to ≈15% of bPEI 25 in the same N:P 5 and 50 µL polyplex volume). These two amines share the same structure, except for two terminal methyl groups. The combination of these two diaminoethane side chains in different ratios in the PSI backbone has been previously compared regarding binding ability and GFP expressing B16BL6 cells[20] showing that tertiary amines may be required for better transfection efficiencies
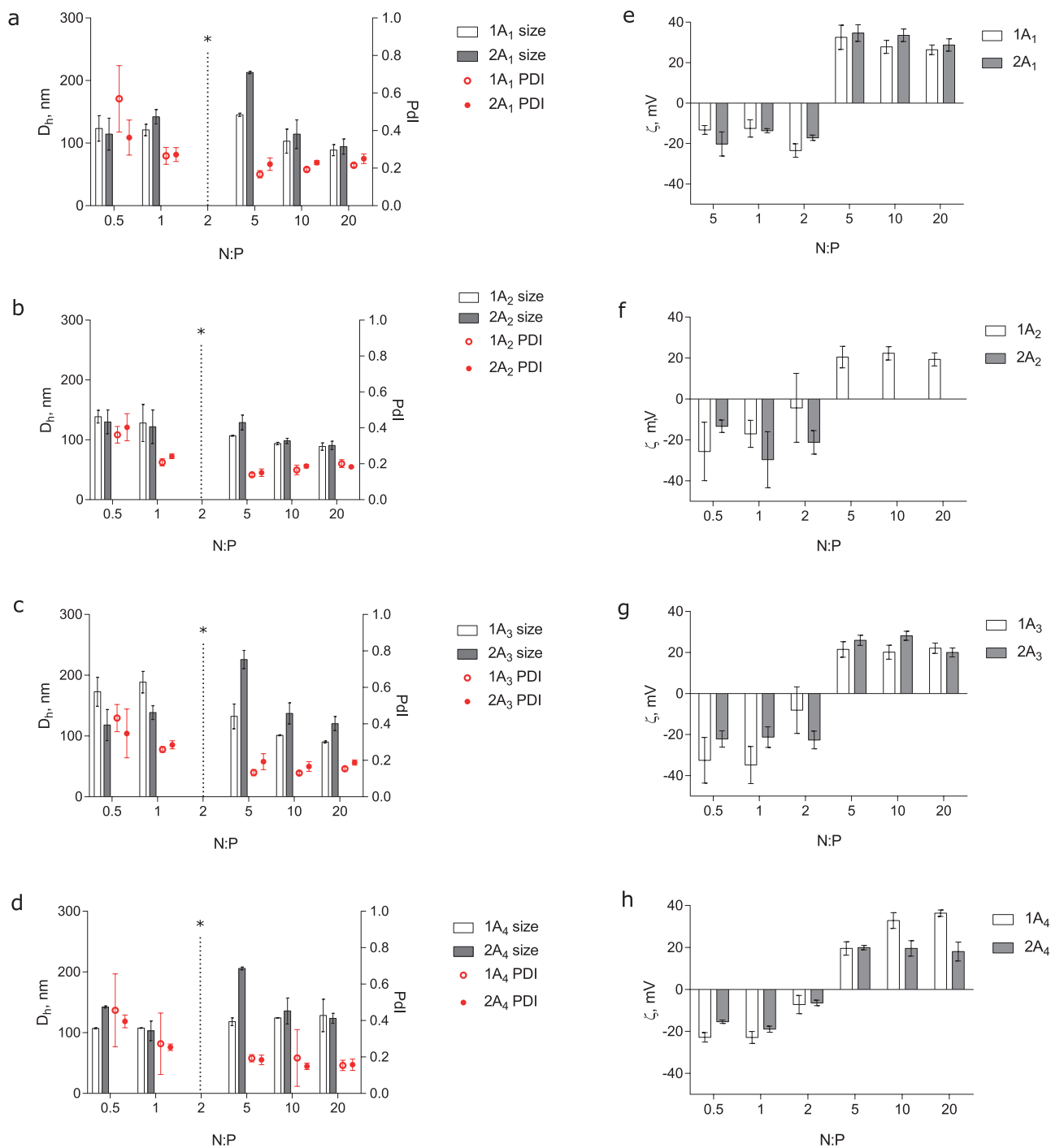
Figure 6. $1A_n$ and $2A_n$ polyplexes with pEGFP-N3: hydrodynamic diameter D_h (nm) and polydispersity index (PDI) by DLS in HEPES buffer at 25 °C. Measurements were performed in triplicate; intensity average mean value is presented. Grid lines with * represent that no data was obtained for the N:P ratio.

as seen for bPEI 25. Here, a slightly higher GFP expressing cells percentage was found in the dodecylated $2A_2$ polycation compared to its non-dodecylated counterpart. The presence of dodecylamine side chain in the PSI backbone of polycation $2A_2$ led to an increased GFP transfection, the opposite behavior of A_1-grafted PSI polycation.

Uchida et al.[53] showed that binding ability and translational efficiency of mRNA of A_1 amine in PSI polyions was comparable to naked mRNA and significantly higher than A_3. Polycations $1A_1$ and $1A_2$ possess two amino groups in the side chain that at pH 7.4 are in double-protonated form in the $1A_1$ ($pk_{a1} = 9.7$ and $pk_{a2} = 8.6$) and single-protonated form in the
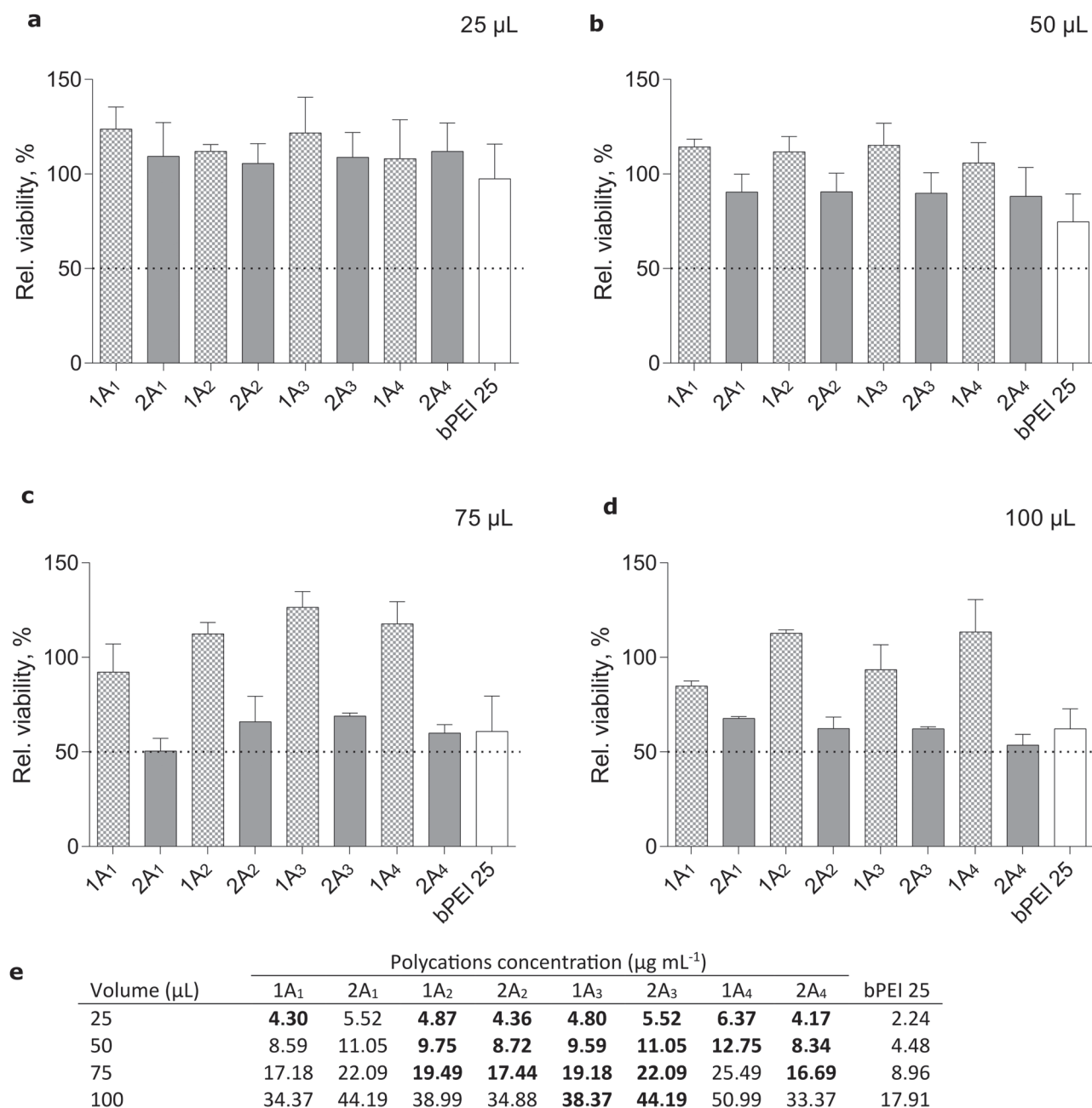
Figure 7. Cytotoxicity of pEGFP-N3/1A$_n$ and pEGFP-N3/2A$_n$ polyplexes at N:P 5 in HeLa cells. Cells were treated with increasing pEGFP-N3/1A$_n$ and pEGFP-N3/2A$_n$ polyplex volumes a) 25 µL, b) 50 µL, c) 75 µL, and d) 100 µL. MTT test was performed after 6 h treatment. Grid line represents 50% relative viability. Error bars represent the s.d. ($n = 3$). e) Final polycation concentration equivalent to polymer volume at N:P 5.

1A$_2$ (pk$_{a1}$ = 9.7), the latter with a tertiary amine with lower pK$_a$ value. Additionally, 1A$_1$ relieves the electrostatic repulsion allowing a double-protonated structure at pH 7.4, an event that probably is undesirable for the higher GFP expressing cells among A$_1$ and A$_2$ polymers, since no protonable amines are available for the endosomal escape inside the cells.

Dodecylated PSI derivatives in the polyplexes pEGFP-N3/2A$_n$ showed stronger binding between the nucleic acid and the polymers, except for pEGFP-N3/2A$_2$ in which the release of DNA occurred with 0.2 to 1 IU of heparin per sample, a range of

heparin concentration that decreased the integrity of polyplex and released the DNA. No release of the DNA from the polyplexes was observed in the range of heparin concentration for all other polyplexes.

In summary, dodecylated polycations provided lower CMC due to the higher polymer–polymer interactions, confirmed by lower molecular mass in the SEC measurements. However, the presence of this alkyl side chain did not interfere in polyplexes size and charges. Indeed, hydrophobization led to higher polymer–DNA interaction possible due to Van der
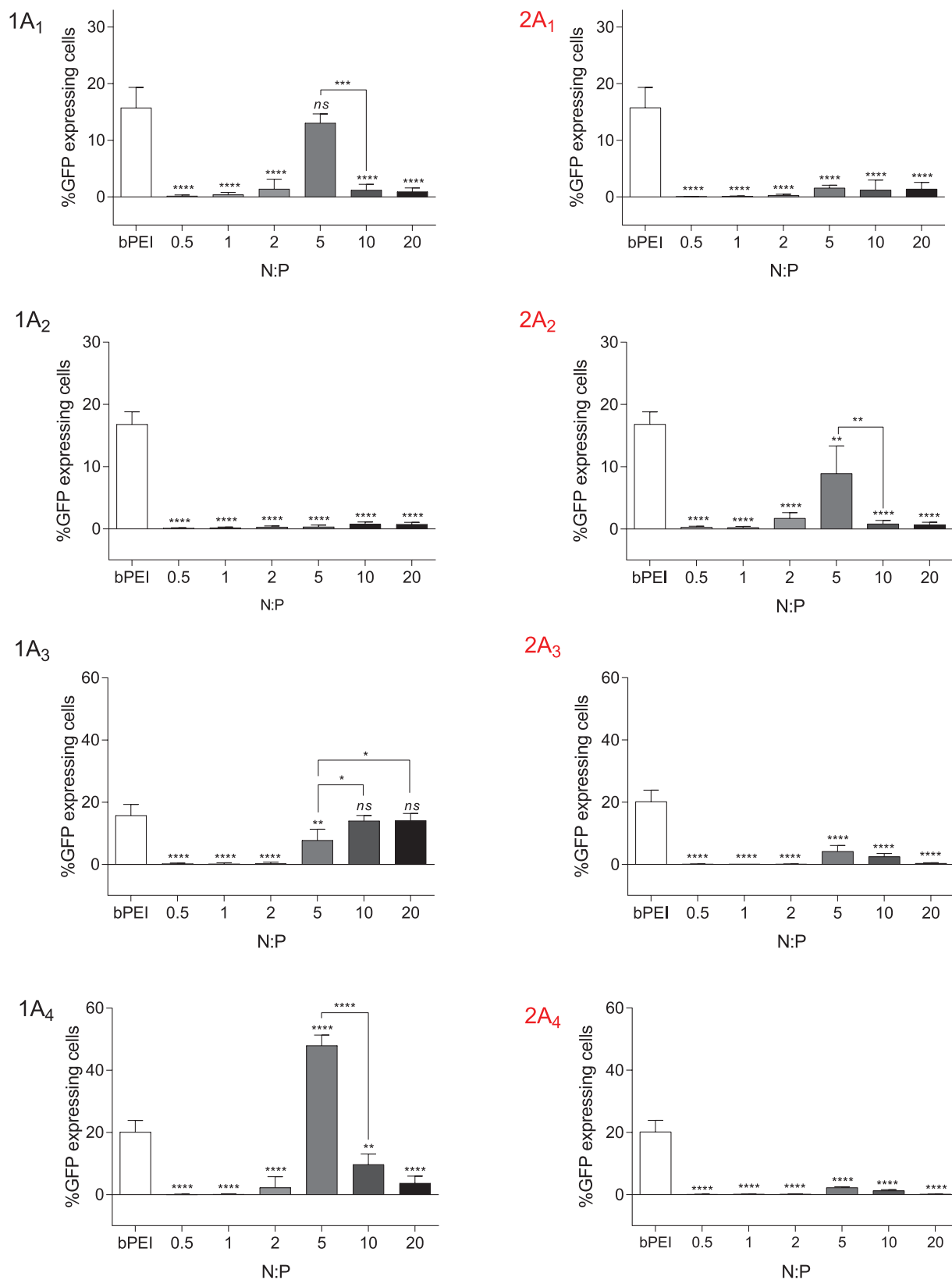
Figure 8. GFP expressing HeLa cells after 48 h treatment with 50 µL pEGFP-N3/$1A_n$ and pEGFP-N3/$2A_n$ polyplexes at different N:P. pEGFP-N3/bPEI 25 polyplexes were used at the same N:P 5 and 50 µL as a positive control. Data are mean ± s.d. ($n = 3$ per group) analyzed by Student's t-test ($n = 3$ per group), all data with Tukey's correction. NS, not significant; $*p < 0.05$, $**p < 0.01$, $***p < 0.005$, and $****p < 0.001$.

**ADVANCED
SCIENCE NEWS**
www.advancedsciencenews.com

**Macromolecular
Bioscience**
www.mbs-journal.de

Waal's interactions associated with the amine-phosphate charge interaction, decreasing transfection presumably due to the lack of intracellular DNA release. Although additional molecular assessments are essential to elucidate details of this mechanism, dodecyl side chains at the backbone of cationic PSI derivatives seem to be indispensable to the stability of polyplexes structures due to the higher binding strength between dodecylated polycations and pEGFP-N3, and may contribute to the protection of pDNA from nuclease attack. In vivo studies may show a different transfection efficiency profile. Increased polymer–DNA interactions via dodecylation may provide in vivo more extended polyplex circulation in blood as well as higher stability toward disassembly mediated by protein corona or even degradation by DNAses.

3. Conclusion

Polycations based on the polysuccinimide structure were synthesized for pDNA delivery. All polymers had lower cytotoxicity in HeLa cells when compared to bPEI 25. Hydrophobization of polycations decreased the critical micellar concentration of all polycations with no changes in the physicochemical properties such as size and charge. Also, GFP expressing cells percentage decreased after dodecylated PSI polyplexes transfection after 48 h. A possible explanation is the hydrophobic interactions between plasmid and the dodecylated polycations via Van der Waal's interactions. With further optimization, it is envisaged that dodecylated polymers may play a role in other lipid-based nanoconstructs and also in co-delivery of genes and other lipophilic drugs.

4. Experimental Section

Materials and Chemicals: L-aspartic acid (ASP), dodecylamine (DDA), N-dimethyldipropylenetriamine (DMAPAPA), bis (3-aminopropyl) amine (norspermidine), triethylenetetramine (DEH), tetraethylenepentamine (TEPA), branched polyethyleneimine 25 kDa (bPEI 25), 1-(3-aminopropyl) imidazole, 1-(2-aminoethyl)piperazine, 3-(4,5-dimethyl-2-thiazolyl)-2,5-diphenyl-2H-tetrazolium bromide (MTT), 4-(2-hydroxyethyl)piperazine-1-ethanesulfonic acid, N-(2-hydroxyethyl)piperazine-N′-(2-ethanesulfonic acid) (HEPES), antibiotics, orthophosphoric acid (H_3PO_4) 85 wt% in water, deuterated solvents (d_6-DMSO, D_2O), N,N-dimethylformamide (DMF), and methanol were purchased from Sigma-Aldrich (Steinheim, Germany) unless otherwise indicated. Water was used as purified, deionized water. As a pDNA vector, pEGFP-N3 from Clontech was used.

Synthesis of Poly(succinimide), (1): Poly(succinimide) (PSI) was obtained according to previously described procedures.[32,36] A thermal polycondensation of L-aspartic acid (ASP) was performed by mixing ASP (10 g, 75.1 mmol) with 12 mol% of orthophosphoric acid 85 wt% (H_3PO_4) (600 µL, 860 mg, 8.8 mmol) using a mortar and pestle. The mixture was taken to an oven at 200 °C, under vacuum, for 3 h. The yellowish crude product was dissolved in N,N-dimethylformamide (DMF), precipitated in methanol, filtered, washed with distilled water.

Synthesis of Poly(succinimide)-co-(N-Dodecamide Aspartate), (2): Here, 10 mol% of dodecylamine (236 µL, 191 mg, 1.03 mmol) were added to PSI (1000 mg, 10.3 mmol) pre-dissolved in dry DMF (5 mL), at 50 °C, and the reaction was kept for 5 h. The reaction mixture was precipitated in distilled water, washed with ethanol, and dried under vacuum at 40 °C for 24 h.

Synthesis of $1A_n$ and $2A_n$ Polycations: Aminolysis of PSI (1) and dodecylated PSI (2) with selected amines. **Figure 9** shows aminolysis of PSI (1) and dodecylated PSI (2), with amines A1–A4. Both 1 and 2 were previously dissolved in DMF and slowly added with a syringe into the amine solutions dissolved in DMF. Reactions were kept for 1 h in an ice bath, then dialyzed with dialyzing tubes with molecular weight cut-off (MWCO) of 3 kDa in water for 48 h, and subsequently lyophilized. The polymers obtained were called $1A_n$ and $2A_n$, according to the side chain amine.

^1H NMR: 30 mg of PSI (1) and dodecylated PSI (2) were dissolved in deuterated DMSO (d_6-DMSO). $1A_n$ and $2A_n$ polycations were dissolved
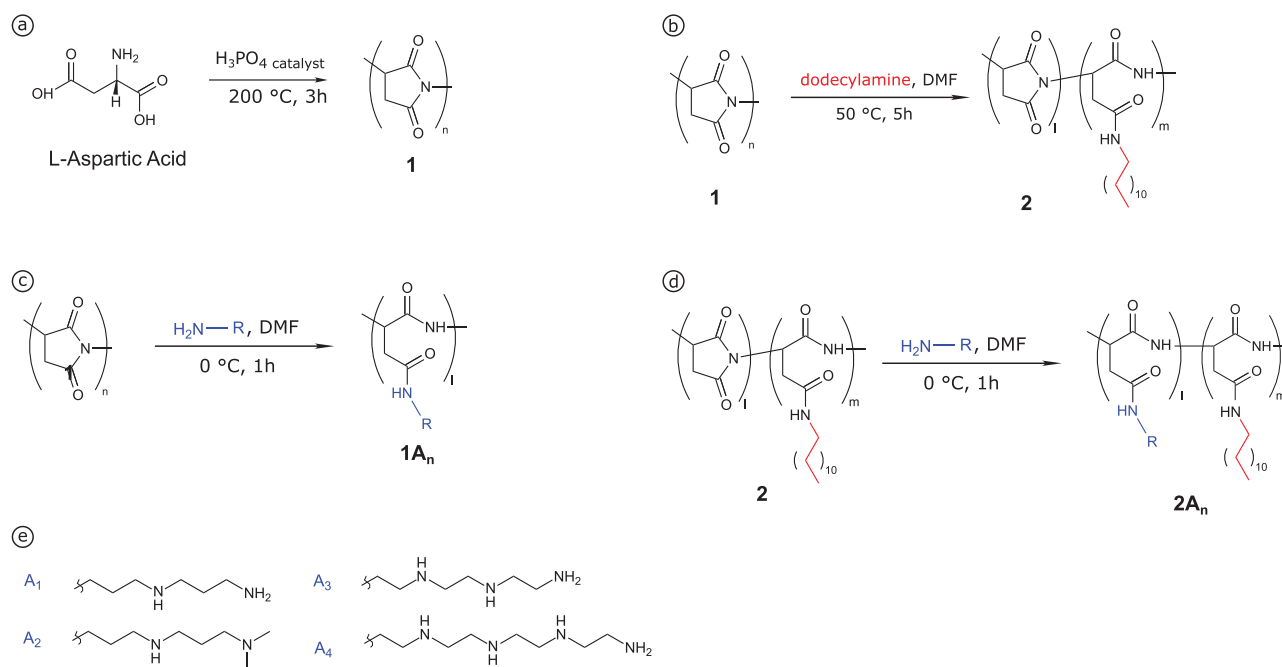

Figure 9. Synthesis of poly(succinimide) (PSI) derivatives. a) Synthesis of PSI (1) from L-aspartic acid (ASP). b) Synthesis of dodecylated PSI (2), degree of substitution (DS) 10 mol%. c) Synthesis of dodecylated PSI (2). d) Synthesis of dodecylated PSI polycations. e) Amines A_n used for aminolysis of 1 and dodecylated PSI (2), obtaining polycations $1A_n$ and $2A_n$.

in deuterated water (D₂O). ¹H NMR spectra were recorded using a Bruker AVANCE III 700 (700 MHz) device. Chemical shifts are reported in ppm and refer to the proper solvent as an internal standard. Data are reported as follows: s, singlet, d, doublet, t, triplet; m, multiplet. Spectra were analyzed using MestreNova by MestreNovaLab Research.

SEC: Number average molecular weight (M_n), weight average molecular weight (M_w), and higher average molecular weight (M_z) of all polymers were obtained from an UltiMate 3000 LC System (Thermo Scientific) with photodiode array (PDA)—UV detector and Shodex RI—101 detector (Showa Denko America, Inc.), with Zenix SEC-100 Sepax column. Sodium acetate 0.3 M, pH 4.40 was used as eluent, and a flow rate of 0.8 mL min⁻¹ and 40 °C were set. The injection volume of the sample was 50 µL. Dextran standards for calibration: Mw 12 kDa, 50 kDa, 80 kDa, 150 kDa, and 670 kDa.

Elemental Analysis (EA), Titration, and Buffering Capacities of Polycations: Elemental analysis of polymers was carried out by VARIO ELIII (Germany) elemental analyzer. For the quantification of protonable amine groups, a titration of all polycations was performed. For this, 10 mg of dry material were dissolved in 30 mL 150 mM sodium chloride (NaCl) solution. pH was adjusted to 12 with 100 mM sodium hydroxide (NaOH) and then the polymers were titrated with 100 mM chloridric acid (HCl) to constant pH 2–3. Equation (1) was used to calculate buffering capacities of all polycations, in which $\Delta(HCl)$ is the volume of acid with concentration C used for the pH change in the range pH 7.4–5.1 and N is the total moles of amine groups in the known amount of polycations.[40]

$$\beta = \frac{\Delta(HCl) \times C(HCl)}{N} \times 100 \tag{1}$$

CMC and Pyrene Fluorescence: CMC measurement was performed on a Jasco FP-6500 with the following settings: λ_{ex} 335 nm, bandwidth 10 nm; λ_{em} 350–550 nm, band width 1 nm; data pitch 0.1 nm; data collection speed of 20 nm min⁻¹; 25 °C. A stock solution of pyrene was prepared using the following procedure: 20 µL of a pyrene solution in methanol (3.5 mM) was evaporated in a 100 mL Erlenmeyer flask; 100 mL of ultrapure water was added and the solution was sonicated for 1 h and afterward filtered through a regenerated cellulose (RC) membrane (0.45 µM). A concentration series of each polymer was prepared using the pyrene stock solution. For each measurement, 1.5 mL were filled into a Quartz cuvette. I_3/I_1-ratio was calculated through the division of the amplitudes at I_3, 385 nm and I_1, 374 nm.

Plasmid Amplification: pDNA was amplified in *E. coli* and purified using a Nucleobond Xtra Midi Kit (Macherey–Nagel). The concentration of plasmid was measured by ultraviolet (UV) absorption at 260 nm. The pDNA purity was assessed by measuring the A_{260}/A_{280} ratios.

Polyplex Formation: Polyplexes were prepared in 350 µL final volume by adding dilutions of polycation in HEPES buffer (20 mM, pH 7.4) into a fixed amount of pDNA dilutions resulting in different N:P ratios (0.5, 1, 2, 5, 10, and 20). N:P value means the ratio between the number of amines of the cationic polymer and the phosphates of the plasmid. Briefly, 131.25 µL of a 0.133 µg µL⁻¹ dilution of pEGFP-N3 in HEPES buffer was transferred to a 500 µL vial, followed by the addition of polymer solution up to 350 µL final volume. For each N:P ratio, the same volume and a constant amount of DNA (17.5 µg) was used.

Electrophoresis Mobility Shift Assay: Agarose gels were prepared by dissolving 1.2 g of agarose in 20 mL of TAE buffer and heated up to 100 °C. After addition of 5 µL of Midori Green Advanced DNA stain for the detection of the nucleic acid, the agarose solution was poured into the electrophoresis chamber. A volume of 10 µL of previously prepared polyplexes were mixed with 5 µL loading buffer and then the mixture added to the gel. Electrophoresis was performed at 120 V for 30 min.

Dynamic Light Scattering (DLS) Measurements—Particle Size and Zeta Potential: 350 µL of polyplexes were prepared and the size measurement was performed on a Malvern Zetasizer ZS in disposable micro UV-cuvettes at 25 °C. Measurements were carried out in the backscatter mode at 25 °C and using a Nd:YAG laser with 532 nm emission wavelength. Samples were prepared with HEPES buffer 20 mM pH 7.4. All samples were measured three times and the size distribution was plotted by intensity distribution. For zeta potential, polyplexes were mixed with a

NaCl solution (NaCl 150 mM final concentration). All experiments were performed in triplicates (mean ± s.d., $n = 3$).

Polyanion Competition Assay: Previously prepared polyplexes were incubated in the presence of the increasing amount of heparin (0, 0.2, 0.4, 0.6, 0.8, and 1 IU per 50 µL polyplex final volume) and incubated for 1 h. Then, 10 µL of polyplexes + heparin were mixed with 5 µL loading buffer and the mixture added to the agarose gel. Electrophoresis was performed at 120 V for 30 min.

Cell Culture: HeLa cells were obtained from Leibnitz Institute DSMZ–German Collection of Microorganisms and Cell Cultures (#ACC 57) and were cultured in in RPMI medium (Thermo Fisher Scientific) supplemented with 10% FBS (FBS Superior, Merck), 1% antibiotics (penicillin and streptomycin), and 1% nonessential aminoacids (NEAA). Cells were cultured in an incubator at 37 °C and 5% CO₂.

Cytotoxicity of Bare Cationic Polymers: Relative viability of HeLa cells for all bare cationic polymer solutions was obtained after 24 h with MTT method. Briefly, cells were plated in a 96-well plate at 1×10^4 cells per well, in 100 µL RPMI containing 10% FBS. After 24 h, cells were treated with a serial dilution of polymers for more than 24 h. Then, the medium was replaced with 200 µL of new medium containing 0.5 mg mL⁻¹ MTT and cells were incubated for 3 h. Wells were replaced with 100 µL isopropanol-HCl and the absorbance measured in Tecan Infinite M200 Pro microplate reader at 570 nm. Relative viabilities were calculated according to the equation $[A]_{test}/[A]_{control} \times 100$, in which A is absorbance and untreated cells served as a control. All experiments were performed in triplicates (mean ± s.d., $n = 3$).

Cytotoxicity of Polyplexes: Relative viabilities of HeLa cells incubated with all polyplexes were obtained after 6 h by MTT assay. Briefly, cells were plated in a 24-well plate at 5×10^4 cells per well, in 500 µL medium containing 10% FBS. After 24 h, cells were treated with 25–100 µL of polyplexes N:P 0.5–20 for 6 h. Then, the medium was replaced with 500 µL of new complete medium containing 0.5 mg mL⁻¹ MTT and cells were incubated for 4 h. Wells were replaced with 200 µL isopropanol-HCl and the absorbance measured in Tecan Infinite M200 Pro microplate reader at 570 nm. Relative viabilities were calculated according to the equation $[A]_{test}/[A]_{control} \times 100$, in which A is absorbance and untreated cells served as a control. All experiments were performed in triplicates (mean ± s.d, $n = 3$).

In Vitro Transfection Efficiency Assay of pEGFP-N3/1A$_n$ and pEGFP-N3/2A$_n$ Polyplexes: HeLa cells were plated in 24-well plates at 5×10^4 cells per well, in 500 µL complete RPMI medium containing 10% FCS, 1% antibiotics, and 1% nonessential aminoacids (NEAA). After 24 h, medium was changed to a 500 µL per well fresh medium without FBS. Then, cells were treated with 25, 50, 75, and 100 µL of previously prepared polyplexes, 500 µL final volume, for 6 h incubation (37 °C and 5% CO₂). Medium was changed to fresh complete medium and after 48 h, cells were washed with PBS and detached with trypsin/EDTA solution. Detached cells were transferred to a flow cytometry tube, centrifuged for 5 min at 140 g and resuspended in PBS. An Accuri C6 (Becton Dickinson, Heidelberg, Germany) flow cytometer and BD Accuri C6 Software were used for the data acquisition. Data was analyzed by FlowJo V10 flow cytometry analysis software. All experiments were performed in triplicates (mean ± s.d., $n = 3$).

Supporting Information

Supporting Information is available from the Wiley Online Library or from the author.

Acknowledgements

Conflict of Interest

The authors declare no conflict of interest.

Keywords

[1] C. F. Jennifer, *Science* **2009**, *324*, 1504.
[2] M. Giacca, S. Zacchigna, *J. Controlled Release* **2012**, *161*, 377.
[3] M. A. Kay, *Nat. Rev. Genet.* **2011**, *12*, 316.
[4] H. Yin, R. L. Kanasty, A. A. Eltoukhy, A. J. Vegas, J. R. Dorkin, D. G. Anderson, *Nat. Rev. Genet.* **2014**, *15*, 541.
[5] A. C. Rinkenauer, S. Schubert, A. Traeger, U. S. Schubert, *J. Mater. Chem. B.* **2015**, *3*, 7477.
[6] T. Wirth, N. Parker, S. Ylä-Herttuala, *Gene* **2013**, *525*, 162.
[7] P. Zhang, E. Wagner, *Top Curr. Chem.* **2017**, *375*, 1.
[8] U. Lächelt, E. Wagner, *Chem. Rev.* **2015**, *115*, 11043.
[9] K. Itaka, K. Kataoka, *Curr. Gene Ther.* **2011**, *11*, 457.
[10] B. Singh, S. Maharjan, T. E. Park, T. Jiang, S. K. Kang, Y. J. Choi, C. S. Cho, *Macromol. Biosci.* **2015**, *15*, 622.
[11] G. Tiram, E. Segal, A. Krivitsky, R. Shreberk-Hassidim, S. Ferber, P. Ofek, T. Udagawa, L. Edry, N. Shomron, M. Roniger, B. Kerem, Y. Shaked, S. Aviel-Ronen, I. Barshack, M. Calderón, R. Haag, R. Satchi-Fainaro, *ACS Nano* **2016**, *10*, 2028.
[12] F. S. Mehrabadi, O. Hirsch, R. Zeisig, P. Posocco, E. Laurini, S. Pricl, R. Haag, W. Kemmner, M. Calderón, *RSC Adv.* **2015**, *5*, 78760.
[13] C. X. He, Y. Tabata, J. Q. Gao, *Int. J. Pharmaceut.* **2010**, *386*, 232.
[14] A. V. Ulasov, Y. V. Khramtsov, G. A. Trusov, A. A. Rosenkranz, E. D. Sverdlov, A. S. Sobolev, *Mol. Ther.* **2011**, *19*, 103.
[15] T. J. Thomas, T. Thomas, *Int. J. Biol. Macromol.* **2018**, *109*, 36.
[16] C. Alvarez-Lorenzo, R. Barreiro-Iglesias, A. Concheiro, L. Iourtchenko, V. Alakhov, L. Bromberg, M. Temchenko, S. Deshmukh, T. A. Hatton, *Langmuir* **2005**, *21*, 5142.
[17] P. Neuberg, A. Kichler, in *Nonviral Vectors for Gene Therapy: Lipid- and Polymer-Based Gene Transfer*, Advances in Genetics, Vol. 88, Academic Press, Amsterdam, The Netherlands **2014**. pp. 263–288.
[18] X. Gu, J. Wang, X. Liu, D. Zhao, Y. Wang, H. Gao, G. Wu, *Soft Matter* **2013**, *9*, 7267.
[19] F. Tanimoto, Y. Kitamura, T. Ono, H. Yoshizawa, *ACS Appl. Mater. Interfaces* **2010**, *2*, 606.
[20] J. Shen, D. J. Zhao, W. Li, Q. L. Hu, Q. W. Wang, F. J. Xu, G. P. Tang, *Biomaterials* **2013**, *34*, 4520.
[21] T. Nakato, M. Tomida, M. Suwa, Y. Morishima, A. Kusuno, T. Kakuchi, *Polym. Bull.* **2000**, *44*, 385.
[22] D. E. Liu, H. Han, H. Lu, G. Wu, Y. Wang, J. Ma, H. Gao, *RSC Adv.* **2014**, *4*, 37130.
[23] J.-H. Yu, J.-S. Quan, J. Huang, C.-Y. Wang, B. Sun, J.-W. Nah, M.-H. Cho, C.-S. Cho, *Acta Biomater.* **2009**, *5*, 2485.
[24] S.-I. Park, E.-O. Lee, J. W. Kim, Y. J. Kim, S. H. Han, J.-D. Kim, *J. Colloid Interface Sci.* **2011**, *364*, 31.
[25] W. Lin, D. Kim, *Langmuir* **2011**, *27*, 12090.
[26] M. Chen, S. P. Jensen, M. R. Hill, G. Moore, Z. He, B. S. Sumerlin, *Chem. Commun.* **2015**, *51*, 9694.
[27] O. K. Appelbe, B. K. Kim, N. Rymut, J. Wang, S. J. Kron, Y. Yeo, *Cancer Gene Ther.* **2017**, *25*, 196.
[28] K. Miyata, M. Oba, M. Nakanishi, S. Fukushima, Y. Yamasaki, H. Koyama, N. Nishiyama, K. Kataoka, *J. Am. Chem. Soc.* **2008**, *130*, 16287.
[29] C. Tros de Ilarduya, Y. Sun, N. Düzgüneş, *Eur. J. Pharm. Sci.* **2010**, *40*, 159.
[30] A. J. O'Keeffe, A. Sigen, D. Zhou, Y. Gao, J. Lyu, Z. Meng, C. Lara, P. Luca, W. Wenxin, *Biomacromolecules.* **2018**, *19*, 1410.
[31] P. S. Kuhn, Y. Levin, M. C. Barbosa, *Physica A, Stat. Mech. Appl.* **1999**, *274*, 8.
[32] H. Chen, W. Xu, T. Chen, W. Yang, J. Hu, C. Wang, *Polymer* **2005**, *46*, 1821.
[33] Z. Y. Ong, C. Yang, W. Cheng, Z. X. Voo, W. Chin, J. L. Hedrick, Y. Y. Yang, *Acta Biomater.* **2017**, *54*, 201.
[34] D. Matulis, V. A. Bloomfield, *Biophys. Chem.* **2001**, *93*, 53.
[35] J. van der Gucht, E. Spruijt, M. Lemmers, M. A. Cohen Stuart, *J. Colloid Interface Sci.* **2011**, *361*, 407.
[36] M. Tomida, T. Nakato, S. Matsunami, T. Kakuchi, *Synthesis (Stuttg)* **1997**, *38*, 4733.
[37] K. Matsubara, T. Nakato, M. Tomida, *Macromolecules* **1998**, *31*, 1466.
[38] B. Khalvati, F. Sheikhsaran, S. Sharifzadeh, T. Kalantari, A. B. Behbahani, A. Jamshidzadeh, A. Dehshahri, *Artif. Cells, Nanomed., Biotechnol.* **2017**, *45*, 1036.
[39] F. Nouri, H. Sadeghpour, R. Heidari, A. Dehshahri, *Int. J. Nanomed.* **2017**, *12*, 5557.
[40] M. Ou, X. Wang, R. Xu, C. Chang, D. A. Bull, S. W. Kim, *Bioconjugate Chem.* **2008**, *19*, 626.
[41] C. Sun, T. Tang, H. Uludag, *Biomaterials* **2013**, *34*, 2822.
[42] B. Thapa, S. Plianwong, K. R. Bahadur, B. Rutherford, H. Uludağ, *Acta Biomater.* **2016**, *33*, 213.
[43] H. Uchida, K. Miyata, M. Oba, T. Ishii, T. Suma, K. Itaka, N. Nishiyama, K. Kataoka, *J. Am. Chem. Soc.* **2011**, *133*, 15524.
[44] R. R. Sawant, S. K. Sriraman, G. Navarro, S. Biswas, R. A. Dalvi, V. P. Torchilin, *Biomaterials* **2012**, *33*, 3942.
[45] A. Dominguez, A. Fernandez, N. Gonzalez, E. Iglesias, L. Montenegro, *J. Chem. Educ.* **1997**, *74*, 1227.
[46] L. Y. Qiu, Y. H. Bae, *Biomaterials* **2007**, *28*, 4132.
[47] S. Roesler, F. P. V. Koch, T. Schmehl, N. Weissmann, W. Seeger, T. Gessler, T. Kissel, *J. Gene Med.* **2011**, *13*, 123.
[48] L. Li, Z.-Y. He, X.-W. Wei, Y.-Q. Wei, *Regen. Biomater.* **2016**, *3*, 99.
[49] G. Roshan Deen, L. H. Gan, Y. Y. Gan, *Polymer* **2004**, *45*, 5483.
[50] K. Seo, D. Kim, *Macromol. Biosci.* **2006**, *6*, 758.
[51] S. Venkiteswaran, T. Thomas, T. J. Thomas, *Chemistry Select.* **2016**, *1*, 1144.
[52] I. Honoré, S. Grosse, N. Frison, F. Favatier, M. Monsigny, I. Fajac, *J. Controlled Release* **2005**, *107*, 537.
[53] H. Uchida, K. Itaka, S. Uchida, T. Ishii, T. Suma, K. Miyata, M. Oba, N. Nishiyama, K. Kataoka, *J. Am. Chem. Soc.* **2016**, *138*, 1478.
[54] S. J. Gwak, C. Macks, S. Bae, N. Cecil, J. S. Lee, *Sci. Rep.* **2017**, *7*, 1.
[55] Z. Shatsberg, X. Zhang, P. Ofek, S. Malhotra, A. Krivitsky, A. Scomparin, G. Tiram, M. Calderón, R. Haag, R. Satchi-Fainaro, *J. Controlled Release* **2016**, *239*, 159.